
Albedo Observations of the Earth's Surface for Climate Research

A. Henderson-Sellers and M. F. Wilson

Phil. Trans. R. Soc. Lond. A 1983 **309**, 285-294
doi: 10.1098/rsta.1983.0042

Email alerting service

Receive free email alerts when new articles cite this article - sign up in the box at the top right-hand corner of the article or click [here](#)

To subscribe to *Phil. Trans. R. Soc. Lond. A* go to: <http://rsta.royalsocietypublishing.org/subscriptions>

Albedo observations of the Earth's surface for climate research

BY A. HENDERSON-SELLERS AND M. F. WILSON
*Department of Geography, University of Liverpool, P.O. Box 147,
 Liverpool L69 3BX, U.K.*

The primary input of energy to the Earth's climate system occurs at the surface and can be highly sensitive to the surface albedo. Albedo changes have been proposed as one cause of climatic variation, but results from climate models are not yet consistent. It is very difficult to establish an agreed global data set with which to initiate comparative climatic simulations. Albedo observations must be spectrally resolved because reflexion of solar radiation is a strong function of wavelength and incident and reflected beams are modified by the atmosphere. Parametrization of system albedos in energy-balance models draws on satellite data. The use of satellite observations is less easy in general circulation climate models. The removal of atmospheric distortion is particularly difficult. The establishment of a surface albedo data set generally follows one of two approaches: geographical categorization or remote monitoring. Surface albedo specification in current general circulation models is diverse. This paper reviews the ways in which remotely derived albedo measurements are used now and may, in the future, be improved for climate research.

1. INTRODUCTION

The majority (over 70%) of the solar energy input to the climate system is first absorbed at the surface (figure 1). Changes in the surface albedo, the ratio of reflected to incident radiation, provide a fundamental source of variability within the climate system. Climate model simulations are sensitive to the input values and parametrization of surface albedo (see, for example, Charney *et al.* 1977; Hummel & Reck 1979; Hansen *et al.* 1981). Globally the absorbed solar radiation, a function of the albedo, α , is balanced by the emitted thermal infrared radiation plus the fluxes of sensible and latent heat, Φ_s and Φ_l (figure 1), so that

$$(1 - \alpha) R_S^\downarrow = e(\sigma T_S^4 - R_L^\downarrow) + \Phi_s + \Phi_l, \quad (1)$$

where e is the infrared emissivity and R_L^\downarrow and R_S^\downarrow downward longwave and shortwave radiation fluxes. The global balance disguises local and regional inhomogeneities.

The reflexion of incident solar radiation from many surfaces is a strong function of wavelength: the albedo of plants is *ca.* 0.10 in the wavelength region below 0.7 μm , rising to *ca.* 0.5 at near-infrared wavelengths, whereas snow is observed to have high albedos *ca.* 0.8 in the visible region, decreasing to *ca.* 0.3 at longer wavelengths (figure 2). Surface albedos are found to depend upon both the incident angle and spectrum of the received radiation and upon the state of the surface (Henderson-Sellers & Hughes 1982). Snow albedo is a function of age, depth, compaction and purity; ice albedos depend upon structure and surface puddling of the ice (Robock 1980; Warren & Wiscombe 1980); the albedo of foliage alters as it matures (Monteith 1973); ocean albedos depend on latitude and wind speed (Cogley 1979) and the albedo of bare soil surfaces is dependent upon the soil moisture (Kondratyev 1969; Ahmad & Lockwood 1979). The considerable range in observed surface albedos makes parametrization

of surface albedo into climate models very difficult. Observational work could be planned better if there were an understanding of the requirements of the modelling community.

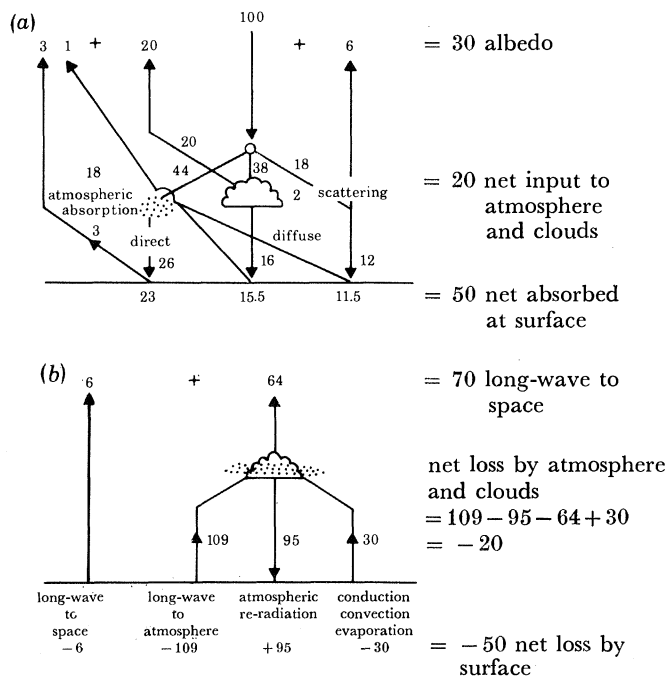


FIGURE 1. Schematic diagram of the globally and annually averaged components of the shortwave (a) and thermal infrared (b) radiation streams.

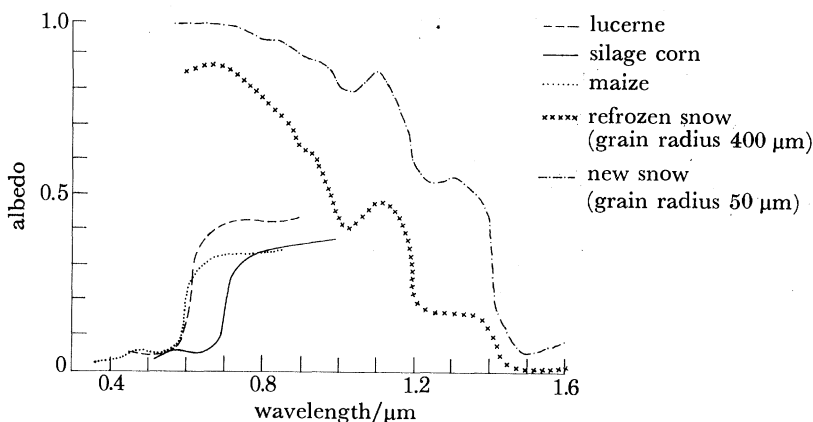


FIGURE 2. Spectral albedos of plant and soil surfaces (data from Kondratyev 1969) and snow albedos (redrawn from Wiscombe & Warren 1980).

2. ALBEDO FOR CLIMATE MODELS

The term albedo implies integration of reflectivity over the full solar spectrum (*ca.* 0.15–1.00 μm). As instruments are frequently restricted to narrow wavelength regions, estimation or calculation (see, for example, Warren & Wiscombe 1980) often replaces integration. The albedo measured by satellites (the system albedo) encompasses surface and atmospheric phenomena (Winston *et al.* 1979). The global albedo is dominated by cloud reflectivity (figure 1).

The method of albedo representation employed varies amongst climate models. The simplest climate models (EBMs) consider an energy balance in latitudinally averaged zones (see, for example, Budyko 1969; Sellers 1969; Cahalan & North 1979; North *et al.* 1981). The albedo parametrization is generally of the form

$$A = \begin{cases} A_{\text{ice}} - f(T(\theta)) & \text{for } T > T_{\text{critical}} \\ A_{\text{ice}} & \text{for } T \leq T_{\text{critical}}. \end{cases} \quad (2)$$

There is no physical basis for parametrization of the system albedo as a function of the surface temperature alone. All other model types include surface and atmospheric reflexion separately. Surface temperature calculations for the averaged globe in one-dimensional radiative convective (RC) models, where the dimension is height, are sensitive to the surface albedo (see, for example, Hummel & Reck 1979; Hansen *et al.* 1981). Statistical dynamical models, formulated in terms of latitude and height, parametrize the energy balance of land and ocean separately within each zone. They also respond to surface albedo changes (see, for example, Potter *et al.* 1975, 1981).

The full three-dimensionality of the climate is parametrized in general circulation models (GCMs). The effects of clouds and atmospheric gases and particulates are treated so that the surface incident radiation is well specified. The surface parametrization includes turbulent fluxes of sensible and latent heat and the radiation term dependent upon the surface albedo. Carson (1981) reviews the land surface albedos used in a wide selection of GCMs. He groups the treatment of snow-free surface albedos into three categories (see table 1): (i) a single fixed value for 'bare' land; (ii) land albedo specified as a function of latitude only; (iii) specified geographical distribution of albedo. The general trend in all GCMs is towards category (iii).

Representation of snow-covered and ice-covered surfaces is diverse, partly because observational data are sparse. The albedo of snow-covered surfaces depends on the type, density and roughness of vegetation and the depth of snow cover (Kukla & Robinson 1980). Snow albedo can increase with cloudiness as a result of near-infrared absorption (Grenfell & Maykut 1977). Carson (1981) identifies three types of snow-covered or ice-covered surfaces (table 1) used in GCMs: (i) surfaces with an instantaneously variable depth of snow either predicted or implied; (ii) permanent or seasonally prescribed snow-covered and ice-covered land surfaces; (iii) permanent or seasonally prescribed areas of sea ice. There is generally a simple dependence of albedo on snow depth (Holloway & Manabe 1971). Since one goal of most modelling groups is to simulate cryosphere-climate feedback, the diversity among the methods of assigning surface albedos and of predicting areas of ice and snow is disturbing. The effect of altering the 'frozen surface' albedo in EBMs (equation (2)) is dramatic (Warren & Schneider 1979; Cahalan & North 1979), whereas GCM simulations of even the present-day cryospheric extent are extremely poor (see §4).

3. GLOBAL SURFACE ALBEDO DATA

The urgent need for an agreed global surface albedo inventory for climate modelling has been identified (see, for example, GARP 1975). There have been a limited number of attempts to produce such a data set but uncertainty over surface albedos persists. The difficulties encountered in trying to construct an acceptable surface albedo data set are considerable. The choice of a 'typical' albedo for a land class from observational data is difficult. Spectral

Downloaded from rsta.royalsocietypublishing.org
TABLE 1. SURFACE ALBEDOS USED IN ATMOSPHERIC GENERAL CIRCULATION CLIMATE MODELS
 (Updated from Carson (1981)).

example centre (reference)	model	snow-free and ice-free surfaces	snow-covered and ice-covered surfaces
Atmospheric Environment Service (Canada) (Boer & McFarlane 1979)	AES	no specific details but implied geographical distribution based on Posey & Clapp (1964)	follows Holloway & Manabe (1971), equation (3): see GFDL
Australian Numerical Meteorology Research Centre (McAvaney <i>et al.</i> 1978)	ANMRC	latitudinal variation based on Posey & Clapp (1964)	snow albedo prescribed as latitudinal variation of α . α of sea ice = 0.07
Computing Centre, Siberian Academy of Sciences (Marchuk <i>et al.</i> 1979)	CCSAS	$\alpha = 0.2$, bare ground $\alpha = 0.1$, ocean	snow: $\alpha = 0.2 + 0.4 d_{sw}$ $\alpha \leq 0.6$ (same as NCAR) ice: $\alpha = 0.6$
Geophysical Fluid Dynamics Laboratory (Holloway & Manabe 1971)	GFDL	geographical distribution based on Posey & Clapp (1964)	snow: equation (3) $\alpha = \alpha_1 + (0.6 - \alpha_1) d_{sw}^{\frac{1}{2}}$ $d_{sw} < 1 \text{ cm}$ $\alpha = 0.6$ $d_{sw} \geq 1 \text{ cm}$ } (3) poleward of 75° lat., albedo for land and pack-ice 0.75
(Manabe & Stouffer 1980)	GFDL	geographical distribution based on Posey & Clapp (1964)	sea ice: 0.5 for lat. < 55°, 0.7 for lat. > 66.5°, 0.45 if top melting
Goddard Laboratory for Atmospheric Sciences (Halem <i>et al.</i> 1979)	GLAS	Feb.: geographical distribution based on Posey & Clapp (1964) Aug.: Charney <i>et al.</i> (1977) vegetated land 0.14, desert 0.35, ocean 0.07	snow and ice 0.70 Holloway & Manabe (1971) equation (3): see GFDL
Goddard Institute for Space Studies (Hansen <i>et al.</i> 1983)	GISS	land: 8 vegetation types have seasonally varying albedos for < 0.7 μm and $\geq 0.7 \mu\text{m}$	snow-free ice: 0.45 ocean, 0.5 land snow albedo: $\alpha_s = 0.5 + e^{-a/5}$ ground partly snow-covered albedo: $\alpha_1 + (\alpha_s - \alpha_1) (1 - e^{-d_{sw}/d_{mask}})$ two spectral regions
Meteorological Office, U.K. (Corby <i>et al.</i> 1977)	UKMO	5-level model: snow-free land values vary with latitude range 0.150–0.223	snow: $\alpha = \alpha_1 + 0.38 d_{sw}^{\frac{1}{2}}$ $\alpha \leq 0.6$ similar to Holloway & Manabe (1971), equation (3): see GFDL sea ice and permanent snow cover: $\alpha = 0.8$; $T_0 < 271.2 \text{ K}$ $\alpha = 0.5$; $T_0 \geq 271.2 \text{ K}$
(Saker 1975)	UKMO	11-level model: land 0.2, sea (where effective) 0.06	transient snow cover 0.5, permanent snow cover, land ice and sea ice 0.8
National Center for Atmospheric Research (Washington & Williamson 1977)	NCAR	originally: geographical distribution based on Posey & Clapp (1964)	originally: snow or ice: $\alpha = 0.2 + 0.4 d_{sw}$ and $\alpha \leq 0.6$
(Dickinson <i>et al.</i> 1981, and unpublished)		third-generation model: two spectral regions < 0.7 μm and $\geq 0.7 \mu\text{m}$; dependence on vegetation type and extent	third-generation model: snow albedo function of age and depth of snow: two spectral regions
Oregon State University (Schlesinger & Gates 1979)	OSU	geographical distribution based on Posey & Clapp (1964) and model's 9 surface types	fixed value
Rand Corporation (Gates & Schlesinger 1977)	RAND	geographical distribution based on Posey & Clapp (1964)	—
University of California at Los Angeles (Arakawa 1972)	UCLA	bare soil 0.14, ocean 0.07	snow-covered 0.7, ice-covered soil or sea water 0.4

Symbols: (i) d_{sw} is the water equivalent depth of snow (centimetres); (ii) a is the snow age (days); (iii) d_{mask} is the vegetation snow masking depth equivalent thickness of water (centimetres); (iv) α_1 is the snow-free land albedo.

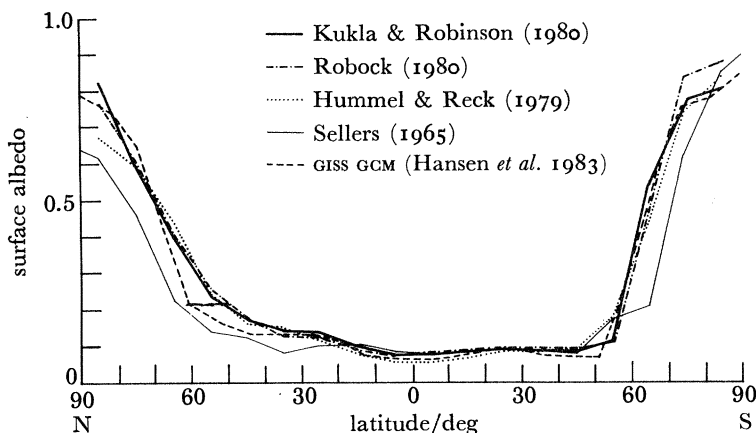


FIGURE 3. Latitudinally averaged cross sections of annual averaged albedos from a variety of sources.

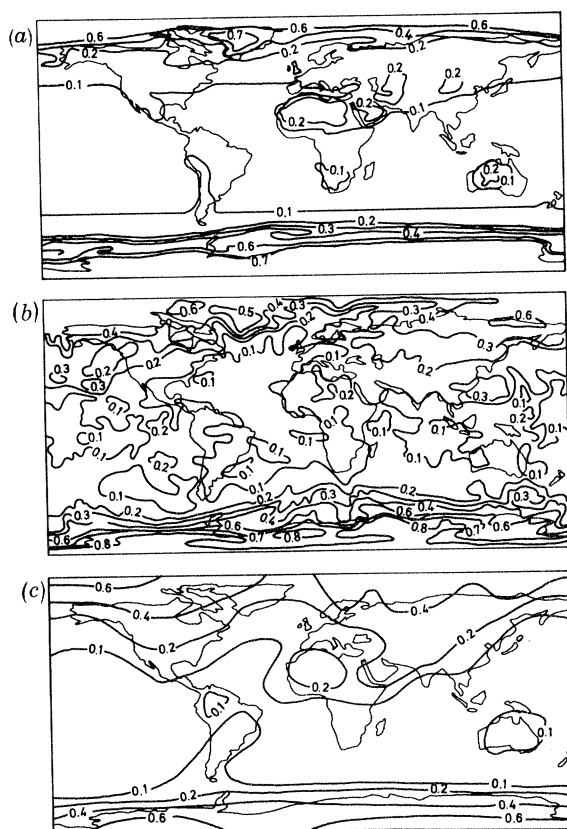


FIGURE 4. (a) GFDL surface albedos (redrawn from Preuss & Geleyn 1980); (b) surface albedos derived from satellite-observed minimum albedos by inversion (after Preuss & Geleyn 1980); (c) surface albedo map drawn from annual average surface albedo values of Hummel & Reck (1979) (from Henderson-Sellers & Hughes 1982).

variation (figure 2), the effects of shading (see, for example, Dozier & Frew 1981; Otterman 1981) and the addition of snow to vegetated environments modify surface albedos. These effects alter as the solar elevation and azimuth vary (Nkemdirim 1973; Ahmad & Lockwood 1979). Atmospheric scatter tends to increase measured clear-sky system albedos. It is therefore preferable to make observations close to the surface. However, satellites may provide the only data in inhospitable areas.

(a) Surveys

There are basically two ways of compiling a surface albedo data set: (i) a satellite data composite; (ii) geographical land type classification plus measurement at selected 'typical' locations. Satellite information alone cannot yet provide acceptable snow and surface albedo data and will never be able to provide information about diffuse surface albedos under total cloud cover. At the high resolution provided by for example Landsat, detailed case studies abound (Moscher & Norton 1977; Rockwood & Cox 1978; Robinove 1982), but a complete global compilation is a massive undertaking. The alternative is to select the lower spatial resolution provided by meteorological satellites. The compilation of a land-surface survey requires the production of a minimum-brightness map (see, for example, Raschke *et al.* 1973). The chance of removing all clouds increases with the time period but so does the 'noise' produced by the surface variability (snow, moisture, vegetation) and the effect of real radiometer noise. Rossow (personal communication 1982) has found that for N.O.A.A. SR data the 3 month absolute minimum value observed has a value approximately 1.6 standard deviations below the true clear-sky minimum. A continually updated minimum albedo will continue to decrease because of instrument noise. In the 'inventory plus specific observation' method of compiling global albedo data there are two problem areas: (a) composing the global classification and (b) obtaining appropriate 'typical' albedo observations for each selected category.

The resulting albedo sets differ (figures 3 and 4). There is a large region of the globe (40° N to 40° S) for which the latitudinally averaged data sets (figure 3) are in agreement. Middle and high latitude values are less consistent. Kukla & Robinson (1980) emphasize the effect of the seasonal cryosphere whereas Hummel & Reck (1979) give greater weight to the seasonality in vegetation albedos. Figure 4 illustrates three global albedo fields. Figure 4a is the global model based on ground and aircraft observations of Posey & Clapp (1964); figure 4b shows surface albedo derived by Preuss & Geleyn (1980) from satellite data calculated by Raschke *et al.* (1973); and figure 4c is the annual albedo map proposed by Hummel & Reck (1979) based on land-survey and ground observations updating the work of for example Posey & Clapp (1964) and Schutz & Gates (1972). In general, low-latitude and mid-latitude values are lower in the satellite-derived data set (figure 4b) over deserts. A greater degree of spatial variation is observed in figure 4b than in either the Hummel & Reck data set (figure 4c) or the Posey & Clapp model (figure 4a). At extreme high latitudes in the Northern Hemisphere the satellite data are lower than surface observations, whereas in the Antarctic satellite derived values are higher than the two ground based data sets. Contamination of the satellite data appears to have been caused by cloud cover in a number of areas.

A major advantage in using satellite-derived data for climate models is that this albedo is ready-integrated information for the grid box sampled. Careful interpretation of satellite data could solve the problem of heterogeneous land classes within a specified GCM grid. However, there are clearly significant discrepancies between surface and satellite-derived data sets.

(b) Limitations of data sets

There are three categories of effects that lead to discrepancies between different observations of surface albedos: (i) instrumental, (ii) viewing geometry, and (iii) environmental, especially atmospheric, influences. Instrumental limitations in satellite surveys result from deficiencies in the optical system, satellite instability, sensor design and degradation, and the orbital configuration. Radiometers not subject to in-flight recalibration drift from their original settings

(see, for instance, Winston *et al.* 1979). The influence of the waveband of the sensor upon the observations can be critical, and comparison of measurements made in different wavelength regions is difficult (see, for example, Duggin *et al.* (1982) and the discussion of figure 5*b*). It is generally found that minimum clear-sky albedo occurs at midday (Nkemdirim 1973). Kowalik *et al.* (1982) give an analysis of the relation between Landsat observed radiances and the solar

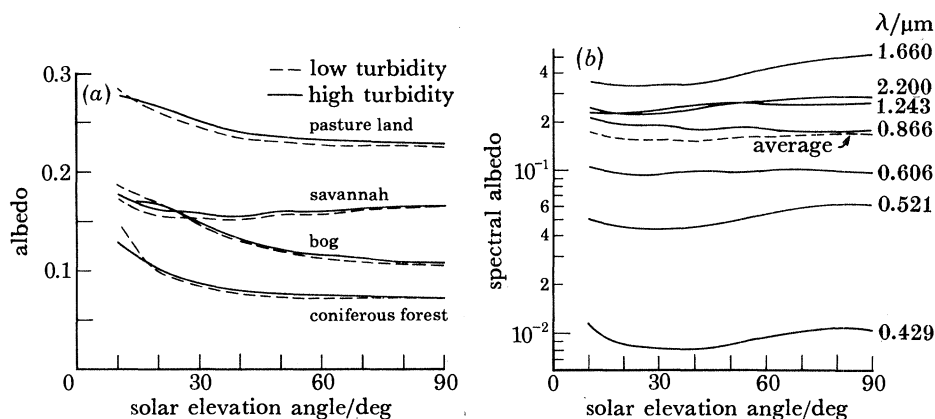


FIGURE 5. (a) Four natural surface albedos, wavelength-integrated from observations for low and high turbidity atmospheres as a function of solar elevation angle (after Kriebel 1979); (b) spectral albedos and wavelength-integrated albedo for savannah as observed on 10 August 1971 (after Kriebel 1979), with permission of Elsevier Science Publishing Co.

zenith angle at the time of observation for ten sites in Nevada. Although significant, the zenith angle effect poses less of a problem for Landsat data than for those data from meteorological satellites.

The non-Lambertian nature of land surfaces (Stowe *et al.* 1980; Kimes & Kirchner 1982) and the influence of the scene geometry upon observed albedos can be considerable (Monteith 1959; Idso *et al.* 1975). Dirmhirn & Eaton (1976) suggest that the reflectance observed through a small aperture, as by satellites, can be inverted from the observed system albedo only if the degree of non-isotropy is known. However, Ueno (1981) suggests that over a complete canopy and mixed surface types, the anisotropic reflective properties of individual elements may be masked and the assumption of isotropy reasonable. Dozier & Frew (1981) and Otterman (1981) derive relations between planar and non-planar configurations. Kriebel (1976) shows that, for low solar zenith angles, shadowing effects are small and that only slight azimuthal anisotropy occurs.

The problem of removal of atmospheric contamination (figure 5*a*) (Turner 1978; Otterman *et al.* 1980) is important for all except very low-altitude flight measurements (Kung *et al.* 1964). Bauer & Dutton (1962) demonstrated that albedo measurements made up to heights of approximately 300–400 m are within 0.05 of measurements made at the surface. This difference is as large as the contrast between some land type classes. Recent theoretical calculations by Briegleb & Ramanathan (1982) illustrate some features of clear-sky albedos and their relation to surface albedos. Duggin *et al.* (1982) show that removal of cloud contamination is difficult. Kriebel (1976, 1979) considers the effect of aerosol loading on satellite-sensed 'clear-sky' albedos. His results suggest a greater dependence upon solar zenith angle than upon atmospheric turbidity (figure 5*a*). Figure 5*b* shows that there is a dependence of spectral albedo upon zenith angle. It seems to be fortuitous that the dependences cancel when the wavelengths are integrated.

The purpose and skill of the originator of the albedo file can be important: cloud contamination, ignored in the original because of detailed local knowledge, may be archived. Moscher & Norton (1977) publish an estimate of the error on their calculated values of surface albedo (*ca.* 11% of the retrieved surface albedo). It is apparent that all current surface albedo data sets should be treated cautiously.

4. CONCLUSIONS AND RECOMMENDATIONS

The effect of incorrect specification of surface albedos upon climate model sensitivity is difficult to ascertain. Hummel & Reck (1979) state that surface albedo errors of ± 0.025 produce uncertainties of ∓ 2.5 K in the surface temperature. Hansen *et al.* (1981) calculate, from their one-dimensional RC model, a temperature change of 1.3 K for a land-surface albedo alteration of 0.05. Sagan *et al.* (1979) calculate a man-generated temperature change of 0.2 K resulting from an albedo change of 0.001 over the last 25 years. Their results have been disputed by Potter *et al.* (1981). Revised calculations suggest that Sagan *et al.* (1979) tend to overestimate the surface albedo by neglecting the recovery of some arid areas. Inclusion of these revisions leads to a global albedo increase of only half that computed by Sagan *et al.* (1979), with a resultant temperature decrease of *ca.* 0.1 K.

The sensitivity of current GCMs to surface albedo changes is a function of the type of change, its geographical location and the nature of the GCM itself. The parametrization of surface albedo in GCMs differs (§2 and table 1). Preuss & Geleyn (1980) make a comparison between very short (10 day) atmospheric integrations by using the surface albedo data sets in figure 4*a, b*. They observe that, although computed surface temperature differences were small, at the cessation of their experiment the atmospheric column temperature showed no tendency to equilibrate.

There are two regions for which GCM climate sensitivity to surface albedo changes has been established: deserts and the cryosphere. In 1975 Charney proposed a biogeophysical feedback mechanism as the cause of extending drought regions in the Sahel. Increased albedo, resulting in a net radiative loss, produced general subsidence, which decreased cloud formation and rainfall (Charney 1975; Charney *et al.* 1977; Sud & Fennessey 1982). It is unclear how surface modification will modify the local climate régime in humid regions. Preliminary results from a simulation of the effects of tropical deforestation in the Amazon region with the GISS GCM show no significant alteration in local or regional surface temperature, although local annual precipitation decreases by 200 mm. The ice-albedo feedback mechanism is believed to be significant for climatic perturbation on a large number of timescales (see, for example, GARP 1975). It is the fundamental forcing effect on EBMS (equation (2)) and is included in all other climate models (see, for example, Wang & Stone 1980; Manabe & Stouffer 1980), although the lack of success of GCMs in simulating the current sea-ice extent (Manabe & Stouffer 1980) could affect computed temperature sensitivities.

It is important that interchange between the remote-sensing and climate-modelling communities be encouraged. Surface albedo variations, caused by changes in the cryosphere extent and vegetation pattern, have been invoked as important causes of climatic change, but modelling results are not yet consistent and no agreed global data set is available with which comparative simulations can be made. Currently the albedo differentiation and level of accuracy derivable solely from satellite measurements are much lower than those being examined in

climate-sensitivity experiments. The development of understanding of our global environment requires constructive and coordinated development of climatic modelling and satellite and surface observational programmes.

M.F.W. holds an N.E.R.C. studentship; part of this work was undertaken while A.H.-S. was an N.R.C. (U.S.A.) Visiting Research Associate at the Goddard Institute for Space Studies, New York. K. P. Shine, N. A. Hughes and J. Jones are thanked for their help.

REFERENCES

- Ahmad, S. B. & Lockwood, J. G. 1979 *Prog. phys. Geog.* **3**, 510–543.
- Arakawa, A. 1972 *Numerical Simulation of Weather and Climate*, Tech. Rep. no. 7. Met. Dept., U.C.L.A.
- Bauer, K. B. & Dutton, J. A. 1962 *J. geophys. Res.* **67**, 2367–2376.
- Boer, G. J. & MacFarlane, N. A. 1979 In *Report of the JOC Study Conference on Climate Models* (GARP no. 22), vol. 1, pp. 409–460.
- Briegleb, B. & Ramanathan, V. 1982 *J. appl. Met.* **21**, 1160–1171.
- Budyko, M. I. 1969 *Tellus* **21**, 611–619.
- Cahalan, R. F. & North, G. R. 1979 *J. atmos. Sci.* **36**, 1178–1188.
- Carson, D. 1981 In *Report of J.S.C. Study Conference on Land Surface Processes in Atmospheric General Circulation Models, Greenbelt, U.S.A., 5–10 January 1981*, pp. 67–108. World Climate Research Programme, I.S.C.U./W.M.O.
- Charney, J. G. 1975 *Q. Jl. R. met. Soc.* **101**, 193–202.
- Charney, J. G., Quirk, W. J., Chew, S. M. & Kornfield, J. 1977 *J. atmos. Sci.* **34**, 1366–1388.
- Cogley, J. G. 1979 *Mon. Weath. Rev.* **107**, 775–781.
- Corby, G. A., Gilchrist, A. & Rowntree, P. R. 1977 In *Methods in computational physics*, vol. 17, pp. 67–110. New York: Academic Press.
- Dickinson, R. E., Jaeger, J., Washington, W. M. & Wolski, R. 1981 *Boundary subroutine for the NCAR global climate model* (NCAR Tech. Note no. 0301/78-01). Boulder, Colorado.
- Dirmhirn, I. & Eaton, F. D. 1976 In *Proc. Symp. Radiation in the Atmosphere* (ed. H. J. Bolle), pp. 435–437. Garmisch Partenkirchen Scientific Press.
- Dozier, J. & Frew, J. 1981 *Remote Sensing Envir.* **11**, 191–205.
- Duggin, M. J., Schoch, L. & Gray, T. I. 1982 In *Proc. SPIE, Symp. East, Washington, D.C., 6–7 May 1982*.
- GARP 1975 *The physical basis of climate and climate modelling* (GARP Publication Series no. 16). (265 pages.) Geneva: World Meteorological Organization.
- Gates, W. L. & Schlesinger, M. E. 1977 *J. atmos. Sci.* **34**, 36–76.
- Grenfell, T. C. & Maykut, G. A. 1977 *J. Glaciol.* **18**, 445–463.
- Halem, M., Shukla, J., Mintz, Y., Wu, M. L., Godbole, R., Herman, G. & Sud, Y. 1979 In *Report of the JOC Study Conf. on Climate Models* (GARP no. 22), vol. 1, pp. 207–253.
- Hansen, J. E., Johnson, D., Lacis, A. A., Lebedeff, S., Lee, D., Rind, D. & Russell, G. 1981 *Science, Wash.* **213**, 957–966.
- Hansen, J. E., Russell, G., Rind, D., Stone, P., Lacis, A. A., Lebedeff, S., Ruedy, R. & Travis, L. 1983 *Mon. Weath. Rev.* (In the press.)
- Henderson-Sellers, A. & Hughes, N. A. 1982 *Prog. phys. Geog.* **6**, 1–44.
- Holloway, J. L. Jr & Manabe, S. 1971 *Mon. Weath. Rev.* **99**, 335–370.
- Hummel, J. R. & Reck, R. A. 1979 *J. appl. Met.* **18**, 239–253.
- Idso, S. B., Jackson, R. D., Reginato, R. J., Kimball, B. A. & Nakayama, F. S. 1975 *J. appl. Met.* **11**, 109–113.
- Kimes, D. S. & Kirchner, J. A. 1982 *Remote Sensing Envir.* **12**, 141–149.
- Kondratyev, K. Ya. 1969 *Radiation in the atmosphere*. (912 pages.) Academic Press.
- Kowalik, W. S., Marsh, S. E. & Lyon, R. J. P. 1982 *Remote Sensing Envir.* **12**, 39–55.
- Kriebel, K. T. 1976 In *Proc. Symp. Radiation in the Atmosphere* (ed. H. J. Bolle), pp. 445–450. Garmisch Partenkirchen Scientific Press.
- Kriebel, K. T. 1979 *Remote Sensing Envir.* **8**, 283–290.
- Kukla, G. J. & Robinson, D. 1980 *Mon. Weath. Rev.* **108**, 56–67.
- Kung, E. C., Bryson, R. A. & Lenschow, D. H. 1964 *Mon. Weath. Rev.* **92**, 543–564.
- McAveny, B. J., Bourke, W. & Puri, K. 1978 *J. atmos. Sci.* **35**, 1557–1583.
- Manabe, S. & Stouffer, R. J. 1980 *J. geophys. Res.* **85**, 5529–5554.
- Marchuk, G. I., Dymnikov, V. P., Lykosov, V. N., Galin, V. Ya., Bobyleva, I. M. & Perov, V. L. 1979 In *Report of the JOC Study Conference on Climate Models* (GARP no. 22), vol. 1, pp. 318–370.
- Monteith, J. L. 1959 *Q. Jl R. met. Soc.* **85**, 386–392.
- Monteith, J. L. 1973 *Principles of environmental physics*. (241 pages.) London: Edward Arnold.

- Moscher, F. R. & Norton, C. C. 1977 In *3rd NASA Weath. and Climate Rev.* (NASA Pub. no. 2029), pp. 171–175.
- Nkemdirim, L. C. 1973 *Agric. Met.* **11**, 229–242.
- North, G. R., Cahalan, R. F. & Coakley, J. A. Jr 1981 *Rev. Geophys. Space Phys.* **19**, 91–122.
- Otterman, J. 1981 *Adv. Space Res.* **1**, 115–119.
- Otterman, J., Ungar, S., Kaufman, Y. & Podolak, M. 1980 *Remote Sensing Envir.* **9**, 115–129.
- Posey, J. W. & Clapp, P. F. 1964 *Geofisica int.* **4**, 33–48.
- Potter, G. L., Elsasser, H. W., MacCracken, M. C. & Ellis, J. S. 1981 *Nature, Lond.* **291**, 47–50.
- Potter, G. L., Elsasser, H. W., MacCracken, M. C. & Luther, F. M. 1975 *Nature, Lond.* **258**, 697–698.
- Preuss, H. & Geleyn, J. F. 1980 *Arch. Met. Geophys. Bioklim.* **29**, 345–356.
- Raschke, E., Vonder Haar, T. H., Bandeen, R. W. & Pasternak, M. 1973 *J. atmos. Sci.* **30**, 341–364.
- Robinove, C. J. 1982 COSPAR Sess. paper no. 10.2.4., Ottawa, Canada, 31 May–2 June.
- Robock, A. 1980 *Mon. Weath. Rev.* **108**, 267–285.
- Rockwood, A. A. & Cox, S. K. 1978 *J. atmos. Sci.* **35**, 513–522.
- Sagan, C., Toon, O. B. & Pollack, J. B. 1979 *Science, Wash.* **206**, 1363–1368.
- Saker, N. J. 1975 Unpublished Met. Off. Met. 020 Tech. Note no. II/30.
- Schlesinger, M. E. & Gates, W. L. 1979 In *GARP/JOC Study Conf. on Climate Models* (GARP no. 22), vol. 1, pp. 139–206.
- Schutz, C. & Gates, W. L. 1972 *Global climatic data for surface, 800 mb, 400 mb.* The Rand Corporation.
- Sellers, W. D. 1965 *Physical climatology.* (272 pages.) Chicago: University of Chicago Press.
- Sellers, W. D. 1969 *J. appl. Met.* **8**, 392–400.
- Stowe, L., Jacobowitz, H. & Taylor, V. R. 1980 In *Proc. Int. Rad. Symp., Fort Collins, Colorado, 11–16 August.*
- Sud, Y. C. & Fennessey, M. 1982 *J. Climatol.* **2**, 105–125.
- Turner, R. E. 1978 In *Proc. of the Twelfth Int. Symp. on Remote Sensing of the Environment*, pp. 783–793.
- Ueno, S. 1981 In *Processes in marine remote sensing*, vol. 12 (ed. P. J. Vernberg & F. B. Diemer), pp. 452–509. University of South Carolina Press.
- Wang, W.-C. & Stone, P. H. 1980 *J. atmos. Sci.* **37**, 545–552.
- Warren, S. G. & Schneider, S. H. 1979 *J. atmos. Sci.* **36**, 1377–1391.
- Warren, S. G. & Wiscombe, W. J. 1980 *J. atmos. Sci.* **37**, 2734–2745.
- Washington, W. M. & Williamson, D. L. 1977 In *Methods in computational physics*, vol. 17, pp. 111–172. New York: Academic Press.
- Winston, J. S., Gruber, A., Gray, T. I., Varnadove, M. S., Earnest, C. L. & Mannello, L. P. 1979 *Earth atmosphere radiation budget analyses derived from NOAA satellite data June 1974–February 1978*, vols 1 and 2. Washington, D.C.: Meteor. Sat. Lab. NOAA-NESS.
- Wiscombe, W. J. & Warren, S. G. 1980 *J. atmos. Sci.* **37**, 2712–2733.